



ISSN: 0067-2904

Design, coordination behavior, and spectroscopic discussion of new thymine-azo chelate with an investigation of some of their applications

Tabarak Taha Mizher*, Alyaa Khider Abbas

Department of chemistry, College of Science, University of Baghdad, Baghdad, Iraq

Received: 23/10/2024

Accepted: 5/ 5/2025

Published: 30/3/2026

Abstract

The thymine-based azo ligand 5-methyl-6-((4-nitronaphthalene-1-yl) diazenyl) pyrimidine-2,4(1H,3H) dione (NAT) was synthesized by diazotization-coupling reaction at room temperature, with its Ag(I) and Cu(II) complexes, subsequently prepared and characterized. Elemental analyses, thermal analyses, and magnetic and molar conductivity confirmed their electrolytic nature, while spectroscopic techniques (FT-IR, HNMR, and UV-Vis and mass spectrometry) revealed structural details. The result appeared that the metal complexes have the molecular formula $[Ag(NAT)(H_2O)_2]NO_3 \cdot 10H_2O$ and $[Cu(NAT)(H_2O)_2]Cl_2 \cdot 10H_2O$. on the chelating of the ligand (NAT) with metal ions involves the nitrogen donor atom of azo moiety and nitrogen (N1) of pyrimidine moiety which the two complexes have four - coordinated tetrahedral geometry is proposed. The molar conductivity of Ag(I) and Cu(II) complexes appeared with electrolytic properties in nature. When tested as wool fabric dyes, NAT and its complexes displayed vibrant colouration, high durability against abrasion, heat, and washing, and retained a glossy finish.

Keywords: Thymine, Azo dye, coordination compounds, spectroscopic studies, bathochromic shift.

تصميم والسلوك التناسقي والمناقشة الطيفية لمخلب الثايمين-الأزو الجديد مع تقص في بعض تطبيقاته

تبارك طه مزهر*, علياء خضر عباس

قسم الكيمياء, كلية العلوم, جامعة بغداد, بغداد, العراق

الخلاصة

تم تصنيع الليكاند methyl-6-((4-nitronaphthalene-1-yl)diazenyl)pyrimidine-2,4(1H,3H)-dione (NAT) المرتكز على الثايمين، وذلك من خلال تفاعل ازدواج أزوي عند درجة حرارة الغرفة، وتم لاحقاً تحضير وتشخيص معقداته مع أيوني Cu(II) و Ag(I). أكدت التحاليل الأولية، إلى جانب التحاليل الحرارية، والمغناطيسية، والتوصيلية المولارية، والطبيعة الإلكترونية لهذه المعقدات. كما كشفت تقنيات التحليل الطيفي، بما في ذلك FT-IR، ¹H-NMR، UV-Vis، وقياسات مطياف الكتلة (MS)، عن تفاصيل بنيوية دقيقة. أظهرت النتائج أن الصيغ الجزيئية للمعقدات هي $[Cu(NAT)(H_2O)_2]Cl_2 \cdot 10H_2O$ و $[Ag(NAT)(H_2O)_2]NO_3 \cdot 10H_2O$. كما بيّنت النتائج أن الليكاند NAT يتناسق مع الأيونات الفلزنية من خلال ذرتي النيتروجين: نيتروجين مجموعة الأزو ونيتروجين حلقة الثايمين. تشير البيانات إلى أن لكلا المعقدتين بنية رباعية التناسق، مع شكل هندسي مقترح هو رباعي السطوح (tetrahedral). أظهرت قياسات

*Email: thaht33@gmail.com

التوصيلية المولارية أن هذه المعقدات تُظهر خصائص الإلكتروليتات. وعند اختبار الليكاند NAT ومعقدية كمصبغات لأقمشة الصوف، أظهرت النتائج ألوانًا زاهية وثباتية عالية تجاه الاحتكاك، الحرارة، والغسيل، مع احتفاظ العينات ببريقها ولمعانها.

1. Introduction

Azo dyes are currently the most widely produced class of dyes, and their significance in the dye and printing industry is expected to grow even further. Their production involves a simple process of diazotization and coupling. Various methods and adjustments are employed to achieve specific color traits, yields, and particle sizes, enhancing their dispersibility [1]. The popularity of azo dyes is attributed to their simple synthesis, wide range of structural variations, high molar extinction coefficients, cost-effectiveness, and moderate to high resistance to degradation from light and moisture [2]. Synthetic dyes are widely utilized in various industrial processes, where the primary goals are color durability and resistance to physical and chemical breakdown. Azo dyes have been the subject of extensive research because of their impressive thermal and optical properties, which make them suitable for use in optical recording media, toners, ink-jet printing, and oil-soluble light-fast dyes. These dyes are typically vibrant compounds capable of producing intense shades of yellow, red, orange blue, or green, depending on their molecular makeup [3]. In the role of an indicator, an azo dye will change color by either accepting or releasing protons or electrons in the solution through protonation. This color shift is more stable with an increased number of azo groups ($-N=N-$) [4, 5]. As a result, poly azo dyes tend to be more stable and suitable for use as indicators. Ideally, reduced delocalization results in a shift of absorption towards shorter wavelengths (hypochromic shift). The absorption of poly azo dyes can be shifted towards longer wavelengths, known as a bathochromic shift, resulting in a redder appearance of reflected light. The stability of these dyes can be determined by studying the impact of acids or bases on their absorption properties and analyzing their energy levels (HOMO and LUMO) through cyclic voltammetry [6]. The study aims to synthesize and characterize a novel ligand (NAT) and its [Ag (I) and Cu (II)] complexes, while also investigating their dyeing properties on the wool fabrics and studying the ligand (NAT) ability as an indicator in different pH.

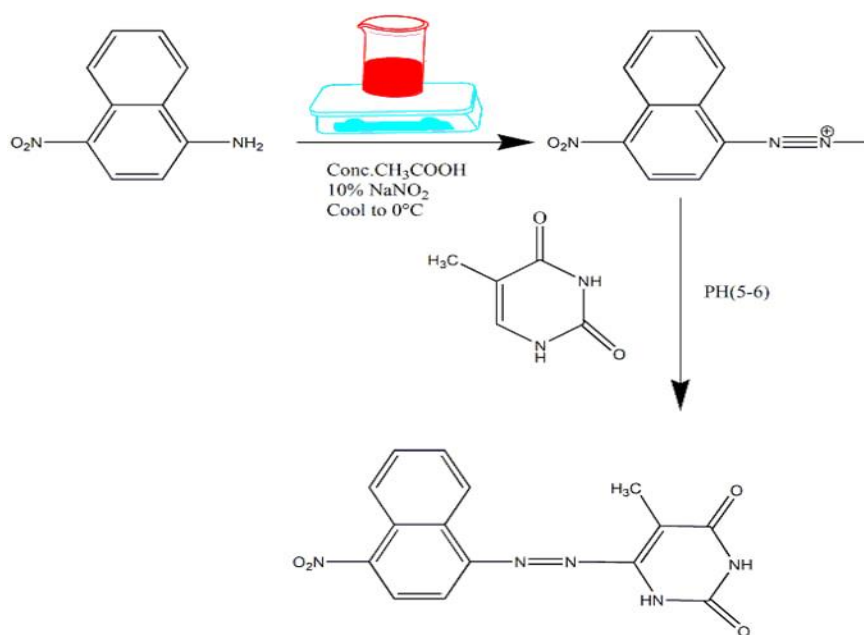
2 Experimental

2.1 material and instrumental

High-purity chemicals and solvents, including thymine, 1-amino-4-nitro naphthalene, sodium nitrate, sodium hydroxide, $Ag(NO_3)$, and $CuCl_2 \cdot 2H_2O$, were employed in the study. All compounds were utilized in their analytically pure forms. The metal content was measured using AAS with a Nova 350.0 spectrophotometer. Infrared spectra ($400-4000\text{ cm}^{-1}$) were recorded using a Shimadzu 8400s spectrophotometer using KBr pellets. The UV-vis spectra were taken using a Shimadzu 1800 UV-vis spectrophotometer. While ^1H-NMR spectra were obtained with a BRUKER AV 400 Avance-III (400 and 100 MHz), and we used DMSO as a solvent. For thermogravimetric analysis (TGA), we used an SDT Q600 V20.9 Build, and the range of decomposition starts from (25-1000) °C. We determined the chloride concentrations in the complexes, whether they were counter-ions or coordinated, using the Mohr method [7]. We measured magnetic susceptibilities at room temperature with a Sherwood Scientific Auto Magnetic Susceptibility Balance. Lastly, we evaluated the molar conductance of the synthesized complexes using a HI9811-5 Hanna instrument.

2.2 Synthesis the ligand 5-methyl-6-((4-nitronaphthalene-1-yl) diazenyl) pyrimidine-2,4(1H,3H) dione (NAT)

The azo ligand (NAT) was synthesized using a process called diazotization and coupling, which was described in other sources [8, 9]. A 10% solution of sodium nitrite (NaNO_2) was mixed with an acidic solution of 4-nitro naphthalene (1.88gm, 0.01mol, 5ml acetic acid, 40ml H_2O) at a temperature of 0-5°C. Then, the cold solution of diazonium acetate was slowly added to a chilled ethanoic-alkaline solution of thymine while stirring for an hour. The resulting orange precipitate was left to settle overnight, then collected by filtration, followed by washing and drying as outlined in [scheme 1].



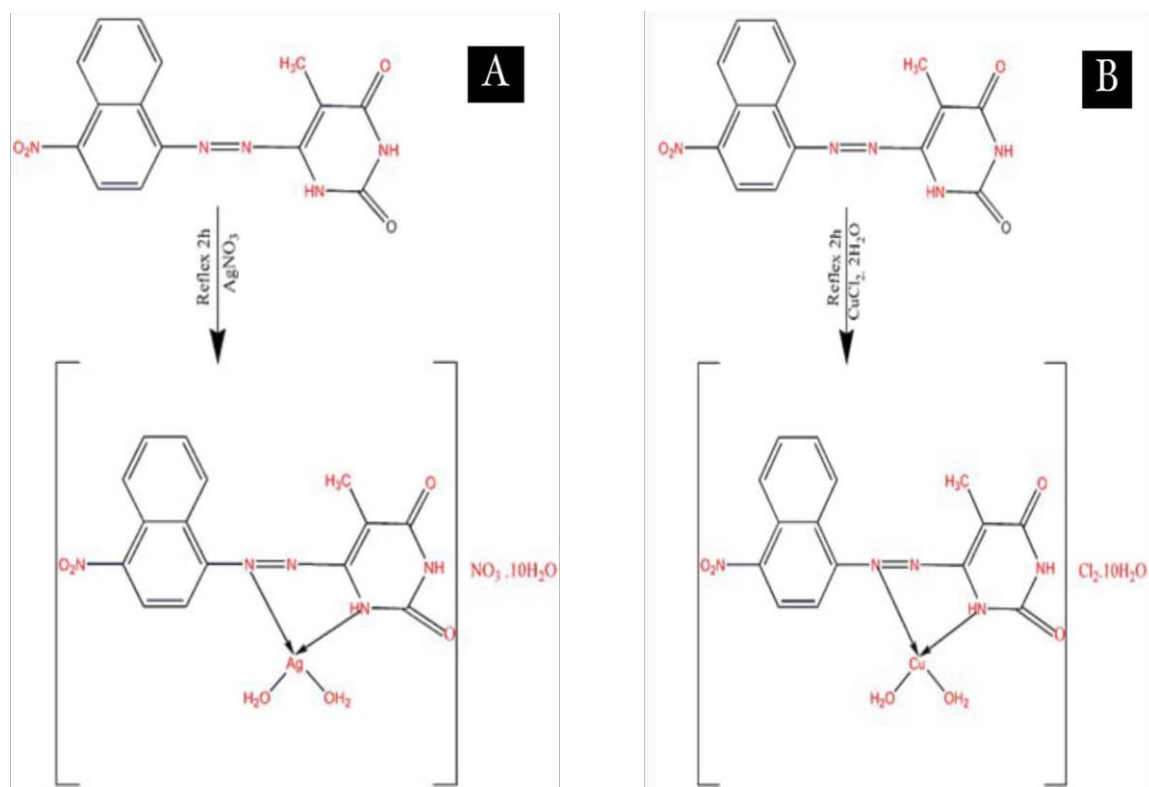
Scheme 1: synthesis of the ligand (NAT)

2.3 Synthesis of the metal complexes

All NAT complexes were synthesized by refluxing an ethanolic solution of the NAT ligand (1 mmol, 0.325 g) with either AgNO_3 (1 mmol, 0.1698 g) or $\text{CuCl}_2 \cdot 2\text{H}_2\text{O}$ (0.170 g) for 2 hours. The resulting solid complexes were filtered wash for several times with a mixture [1:1][dil. Water: EtOH], finally dried and collected. The physicochemical characteristics of synthesized compounds are shown in Table 1.

table 1: physicochemical characteristics of synthesized compounds

No	Compounds (M.wt) (gm/mol)	Color and (λ)max	M:L	Δm (S.mol- 1.	Elemental Analysis				
					Experimental% (Theoretical%)				
					C	H	N	M	Cl
1	NAT ($\text{C}_{15}\text{H}_{11}\text{N}_5\text{O}_4$) (325.0) g/mole	Orange 419nm	-----	20.8	55.33 (54.47)	3.38 (3.07)	21.15 (21.19)	-----	-----
2	$[\text{Ag}(\text{NAT}) (\text{H}_2\text{O})_2]$ $\text{NO}_3 \cdot 10\text{H}_2\text{O}$ (711.11)g/mole	Purple 498nm	1:1	42	25.31 (25.41)	4.92 (3.86)	11.81 (10.91)	14.32 (15.06)	-----
3	$[\text{Cu}(\text{NAT}) (\text{H}_2\text{O})_2]$ $\text{Cl}_2 \cdot 10\text{H}_2\text{O}$ (675.08)g/mole	Orange 453nm	1:1	79	26.63 (27.25)	5.17 (4.89)	10.35 (11.25)	9.11 (11.6)	10.0 10.5



Scheme 2: The synthesis of NAT complexes [A] $[\text{Ag}(\text{NAT})(\text{H}_2\text{O})_2] \text{NO}_3 \cdot 10\text{H}_2\text{O}$ and [B] $[\text{Cu}(\text{NAT})(\text{H}_2\text{O})_2] \text{Cl}_2 \cdot 10\text{H}_2\text{O}$

3 Result and Discussion

3.1 Thermogravimetric analysis (TGA)

Thermal degradation of the ligand (NAT) occurs in four exothermic phases across the temperature range of 25–1000 °C. The first phase of breakdown happened between 25 - 270°C, leading to a weight loss of 4.91%; the second phase, from 270 to 420 °C, with a 17.72% weight loss; the third phase happened between 270 to 570°C, causing a 5.862% loss. Finally, the fourth and last phase, from 570 to 830°C, leads to a significant weight loss of 20.63%. As depicted in [Figure 1(A)], for the $[\text{Ag}(\text{NAT})(\text{H}_2\text{O})_2] \text{NO}_2 \cdot 10\text{H}_2\text{O}$ complex. The thermal decomposition of the compound occurred in distinct stages. The initial step (25 and 110°C) showed a weight loss of 4.083% accredit to the loss of lattice water [10]. Subsequently, the second stage, occurring from 110 to 250°C, results in a 16.47% weight loss. Decomposition phase 250 to 500°C, resulted in an 8.008% weight loss, followed by fourth stage spans 500 to 690°C, with a 13.91% weight reduction. The final degradation step (690–1000°C) demonstrated the most substantial mass loss (33.77%), as illustrated in [Figure 1(B)] [11]. Regarding the $[\text{Cu}(\text{NAT})(\text{H}_2\text{O})_2] \text{Cl}_2 \cdot 10\text{H}_2\text{O}$ complex, decomposition occurs in seven steps as shown in [Figure 1(C)]. The first stage, from 25 to 100°C, results in a weight loss of 3.136%. The second stage observes a 5.543% loss between 100 to 150°C. The third stage, from 150 to 300°C, results in an 8.223% weight loss. The fourth stage, ranging from 300 to 510°C, sees a 16.33% weight reduction; while the fifth stage, between 510 and 690°C, leads to a 7.947% loss. The sixth stage produces a 12.77% weight loss from 690 to 750 °C, and the final step, between 750 and 1000 °C, resulting in a 20.10% weight loss [12]. The results and equations from the analytical data align well with the thermogravimetric analysis, indicating that the degradation of the ligand (NAT) and its complexes happened in multiple stages. See Table 2 for TGA data on the ligand (NAT) and its complexes.

Table 2: TGA data on the ligand (NAT) and its complexes

comp& molecular formula (molecular weight)g/mole	Step	TG Range of the decomposition	suggested fragment	Mass loss%	
				Cal%	Found%
NAT C ₁₅ H ₁₁ N ₅ O ₄ (325)g/mole	1	(25-270) °C	CH ₄	4.91	4.945
	2	(270-420) °C	C ₃ H ₇ N	17.52	17.72
	3	(420-570) °C	C ₁ N ₁	5.840	5.862
	4	(570-830) °C	C ₃ N ₂	18.137	17.94
	5 Residue	(830-1000) °C <1000°C	C ₃ NO C ₄ N ₂ O ₃	20.288 32.90	20.63 32.91
[Ag(NAT) (H ₂ O) ₂]NO ₃ .10H ₂ O Ag C ₁₅ H ₂₃ N ₆ O ₁₉ (711.11)g/mole	1	(25-110) °C	H ₃ O	4.078	4.083
	2	(110-250) °C	H ₅ O ₇	16.45	16.47
	3	(250-500) °C	C ₄ H ₈	9.140	8.008
	4	(500-690) °C	C ₈	13.50	13.91
	5 Residue	(690-1000) °C <1000°C	C ₃ N ₆ O ₃ Ag	33.75 23.75	33.77 23.76
[Cu(NAT) (H ₂ O) ₂] Cl ₂ .10H ₂ O Cu C ₁₅ H ₂₅ N ₅ O ₁₆ (675.08)g/mole	1	(25-100)°C	H ₅ O	3.10	3.136
	2	(100-150) °C	H ₅ O ₂	5.47	5.543
	3	(150-300) °C	H ₇ O ₃	8.138	8.223
	4	(300-510) °C	H ₉ O ₄ Cl	16.27	16.33
	5	(510-690) °C	Cl O	7.694	7.947
	6	(690-750) °C	C ₆ O	12.42	12.77
	7 Residue	(750-1000) °C <1000°C	C ₉ N ₂ CuN	19.53 25.94	20.10 25.95

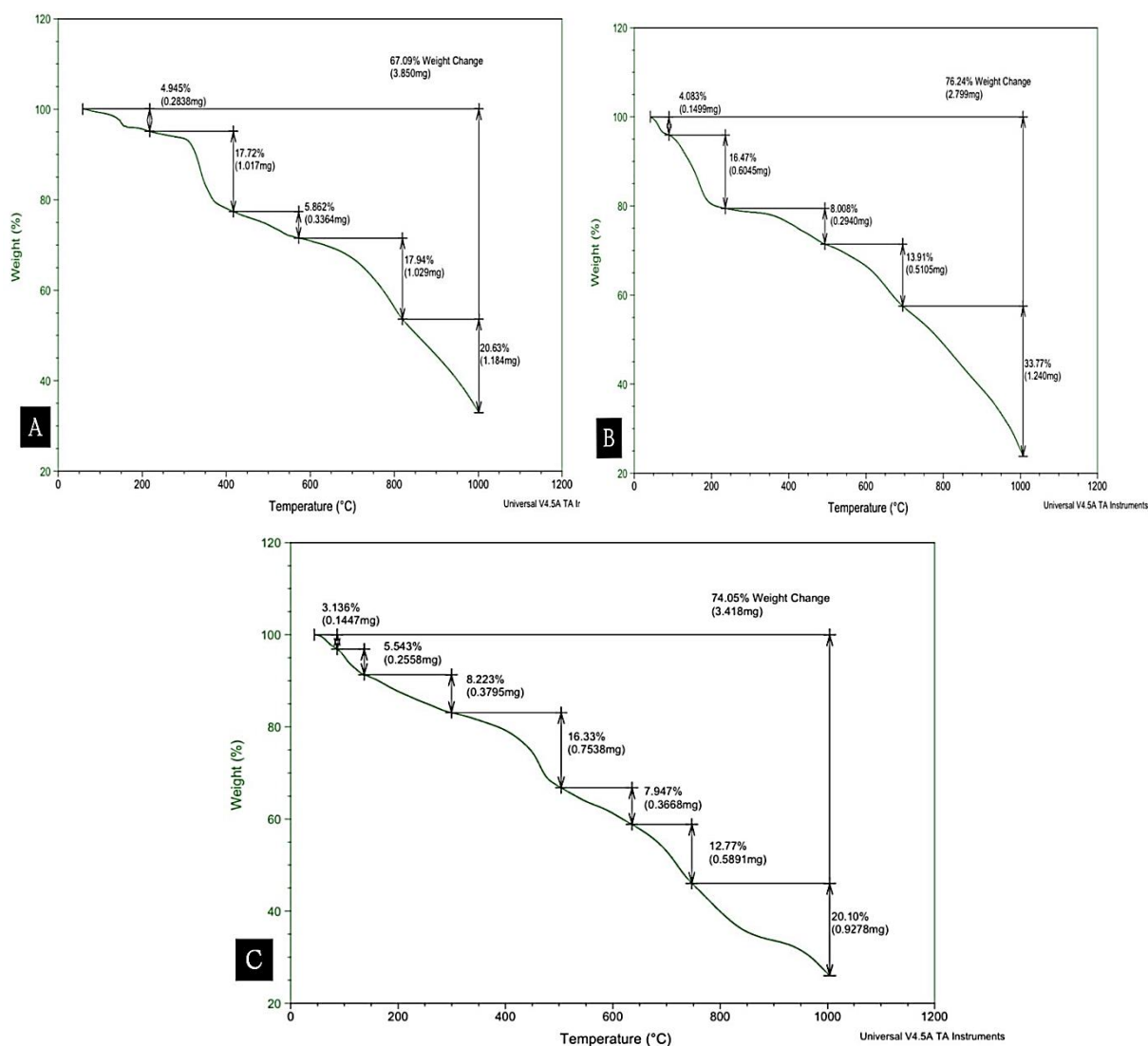
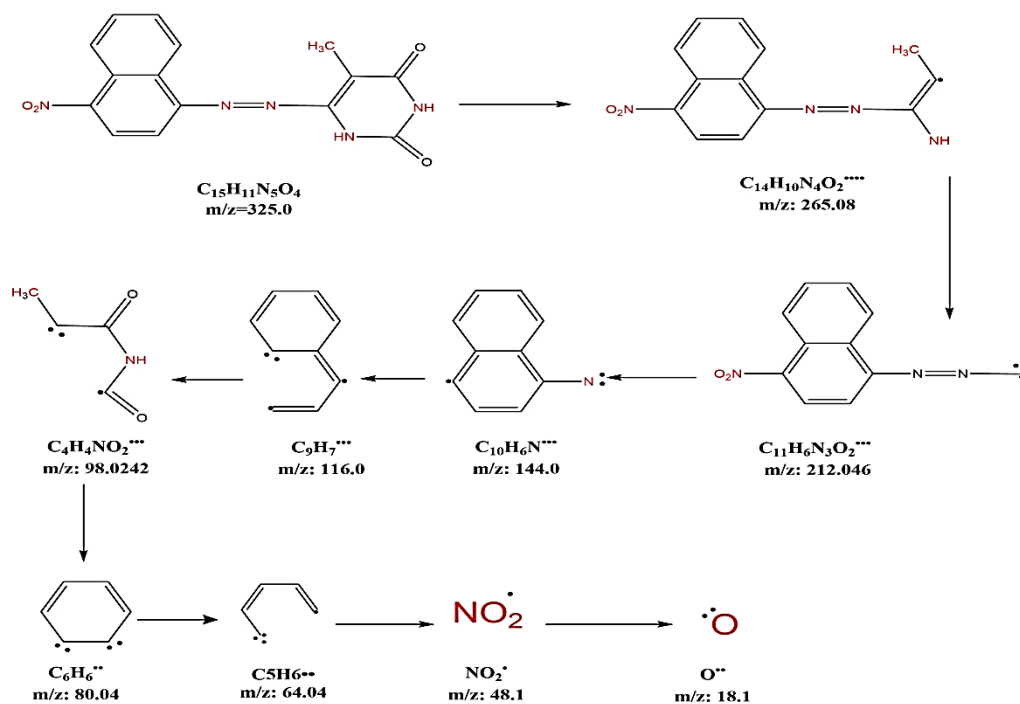


Figure 1: Thermal disintegration of (A) NAT ligand (B) $[\text{Ag}(\text{NAT}) (\text{H}_2\text{O})_2]\text{NO}_3 \cdot 10\text{H}_2\text{O}$ (C) $[\text{Cu}(\text{NAT}) (\text{H}_2\text{O})_2] \text{Cl}_2 \cdot 10\text{H}_2\text{O}$

3.2 Mass spectrometry

Mass spectrometry serves as a powerful analytical technique for both qualitative and quantitative analysis. The suggested molecular formula of the NAT ligand was emphasized by the different obtained molecular ion peaks at various intensities, base peaks, and other fragments. As illustrated in scheme 3 and Figure 2, the molecular ion peak at $m/z = 325.0$ confirmed the formation of the ligand NAT, and the base peak was found at $m/s = 80.0$ with highly intense [13].



Scheme -3 Shows the most characteristic fragments of (NAT) ligand.

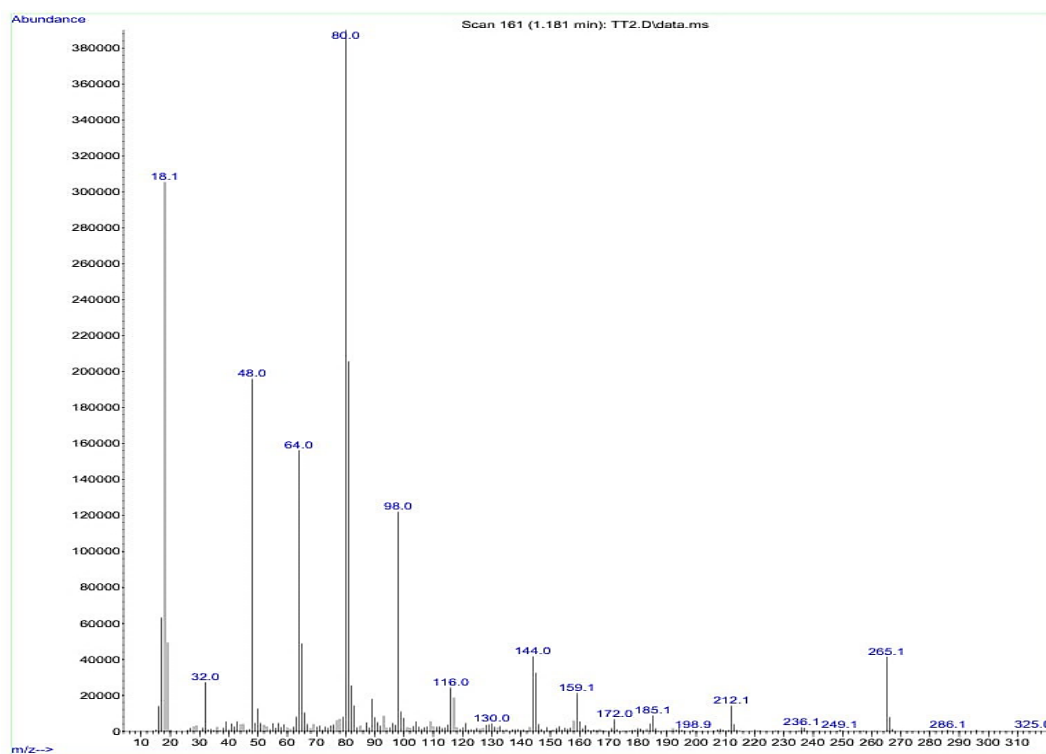


Figure 2: mass spectrum of (NAT) ligand

3.3 The Electronic spectroscopic and magnetic measurement

The electronic absorption spectra of the ligand (NAT) and its [Ag(I) and Cu(II)] complexes were recorded at the range (200-1100)nm with $[10^{-4}M]$ in ethanol as a solvent. All data was represented in the Table (3) and Figure (3A-C) [14]. A spectrum of the ligand NAT

displays bands at (289 nm, 34602 cm^{-1}) and (419 nm, 23866 cm^{-1}) due to $\pi \rightarrow \pi^*$ and $n \rightarrow \pi$ transition of aromatic and heterocyclic moieties as well as the carbonyl and azo group respectively [15, 16]. on the other Ag (I)-NAT Figure 3(B) appeared as a doublet at (498nm, 20080 cm^{-1}) and (440nm, 22727 cm^{-1}) which was assigned to a charge transfer (CT) which has a dia magnetic [17]. The electronic absorption spectrum of Cu (II)-NAT complex [figure 3(c)] appeared with an absorb band at (453nm, 22072 cm^{-1}) due to the ${}^2T_2 \rightarrow {}^2E$ transition of tetrahedral geometry, which was integrated with charge transfer. So, the magnetic susceptibility value [1.78] = lies within the range notify for (d^9) ion Cu (II) [18].

Table 3: Electronic spectra information of the ligand (NAT) and its complexes.

Compounds	(nm)	Wave number (cm^{-1})	Assignment	Hybridization	Geometry	μ_{eff} (B.M)
(NAT)	289 419	34602 23866	$\pi \rightarrow \pi^*$ $n \rightarrow \pi$	-----	-----	-----
[Ag(NAT)(H ₂ O) ₂]NO ₃ .10H ₂ O	440 498	20080 22727	CT	sp ³	Tetrahedral	Dia
[Cu(NAT)(H ₂ O) ₂] Cl ₂ .10H ₂ O	453	22075	${}^2T_2 \rightarrow {}^2E$	sp ³	Tetrahedral	1.78

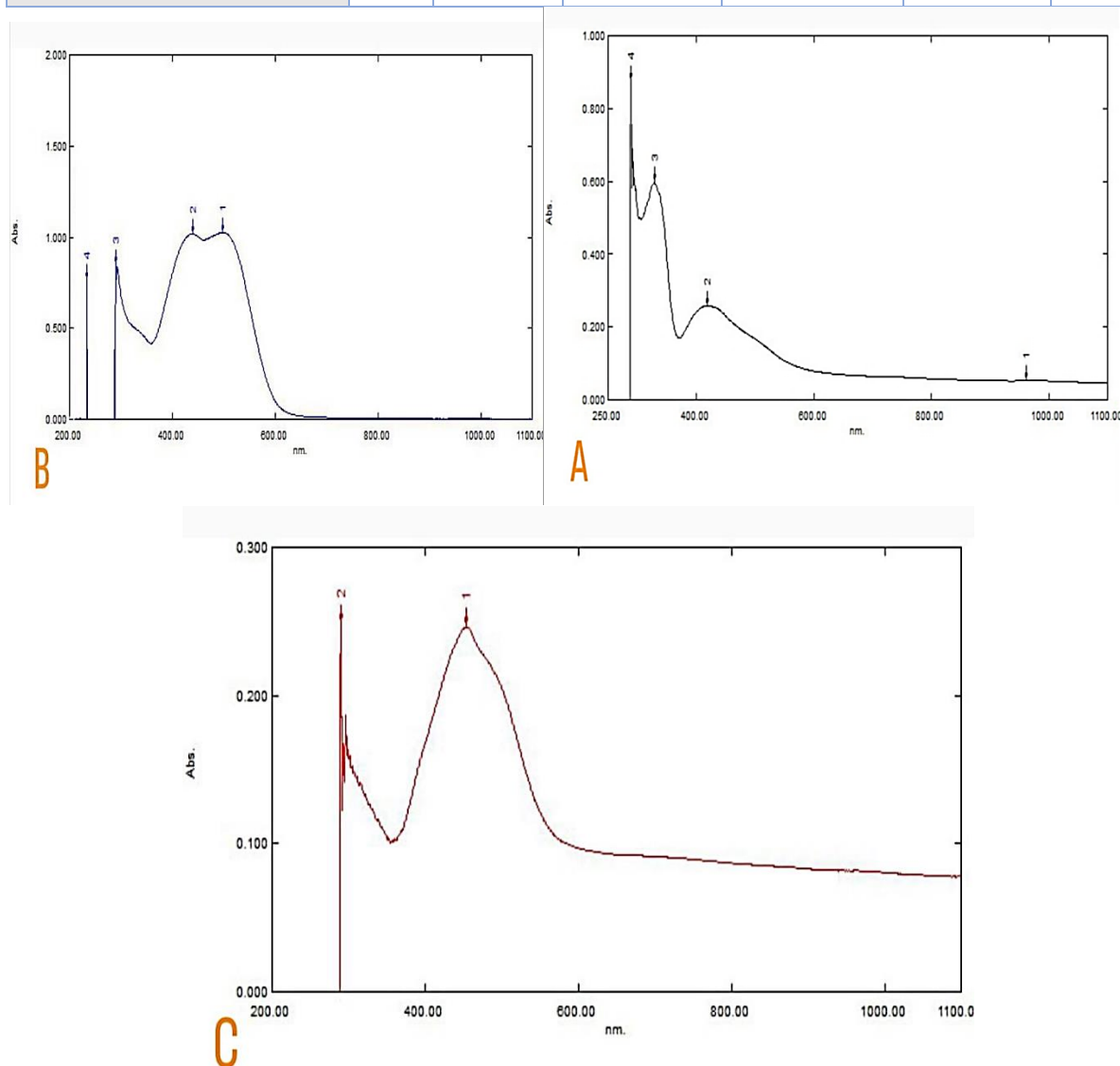


Figure 3: electronic spectra of (A) NAT ligand (B) [Ag(NAT) (H₂O)₂] NO₃.10H₂O (C) [Cu(NAT) (H₂O)₂] Cl₂.10H₂O

3.4 The FT-IR spectra of ligand NAT and its complexes

A comparative analysis of the FT-IR spectra was conducted to elucidate the binding mode of the NAT ligand with metal ions in the complexes. The spectra showed bands related to the ligands, with some differences because of the chelation process. The majority of the molecules' vibrations were conducted utilizing KBr pellets between 400 and 4000 cm^{-1} , as Figure 4 illustrates. The N (C-N) in the thymine moiety is assimilated to the band at 1353 cm^{-1} in the NAT ligand spectrum [19, 20]. This band's cooperation with the metal ion caused changes to its position and form. The stretching vibration band of the carbonyl group remained unchanged in the spectra of the complexes [figure 4 (B and C)], Although no chelating happens through these moieties[21, 22], Sometimes, small shifts in position or shape were thought to be caused by changes in resonance because of chelation [23, 24]. Azo compounds exhibit separate feature bands (N=N)[25]. The NAT ligand's spectra show a band at [1442 and 1477] cm^{-1} . However, C-N=N-C has stretching absorption in [1247,1174] cm^{-1} . Chelation decreases the positioning and strength of these bands in complex spectra [Table 4] [26, 27]. The FT-IR spectra of the complexes revealed new absorption bands absent in the free NAT ligand spectrum, with particularly significant shifts observed in the 405-622 cm^{-1} . These new bands likely correspond to M-N_{azo}, M-N_{imidazole}, and M-O_{H₂O} stretching. This helps support our idea of where the ligands attach to the metal ions. This shows that the NAT ligand works as a neutral N, N-bidentate ligand [28, 29].

Table 4: Vibration bands for ligand (NAT) and its complexes.

Compounds	ν OH Lattice (coordinate)	ν NH	ν C=O	ν C-N-	ν N=N	ν C- N=N- C	ν M- NH Prm.	ν M- N AZO	ν M-O H ₂ O
NAT	-----	3076 3047T 3020	1614 1575T.	1353s h	1442 1477	1247 1174d, sh	-----	-----	-----
[Ag(NAT)(H ₂ O) ₂] ₂ NO ₃ .1 0H ₂ O	3446 T 3456	3107 3147d,v w	1649 1629d, m	1379 1359d, st	1465m	1253 1203 1163 T,st	690 m	580 w	422d, w
[Cu(NAT)(H ₂ O) ₂] ₂ Cl ₂ .10 H ₂ O	3460T	3002V w	1649 1600	1359v w	1500 1471d, st	1249 1193d, st	690 sh	595 w	455 vw

s= strong m= medium, w= weak, sh= sharp, prm= pyrimidine, imd= imidazole, pyr= pyrazole, T= tall, d= double

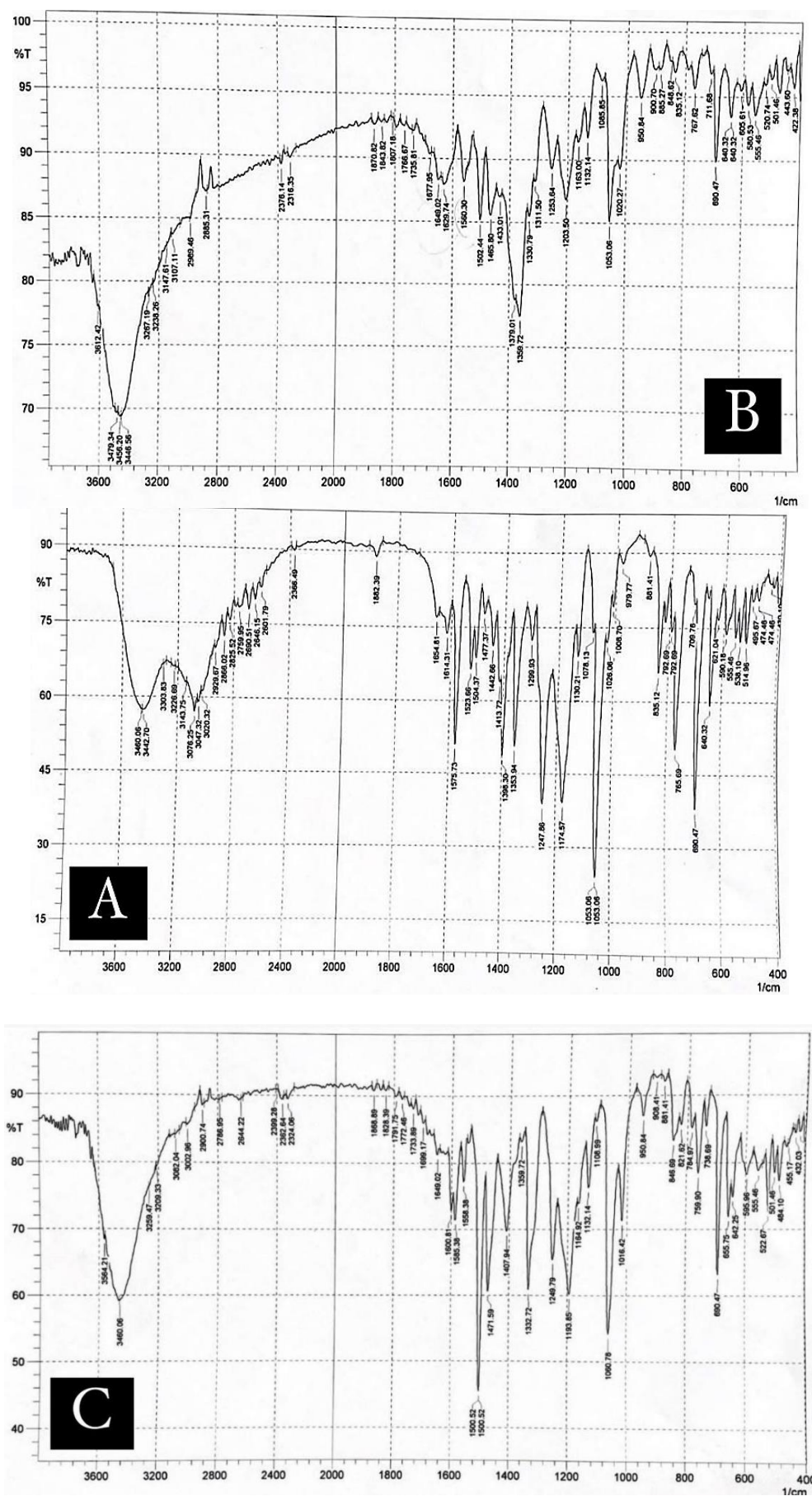


Figure 4: The FT-IR for (A) NAT ligand (B) $[Ag(NAT)(H_2O)_2]NO_3 \cdot 10H_2O$ (C) $[Cu(NAT)(H_2O)_2]Cl_2 \cdot 10H_2O$

3.5 ^1H NMR spectra of the ligand NAT

Table 5 provides the chemical shifts (δ) in ppm for different types of protons in the ligand (NAT), while [Figure 5] displays the ^1H NMR spectrum of the ligand NAT. The singlet signal observed at (8.81) ppm is assigned to the δ (NH, H) of thymine, and the signal at (1.72) ppm corresponds to the δ (3H, CH_3) of the thymine moiety [30]. Multi signals were observed in (7.32-7.70) ppm was attributed to the proton of the naphthalene ring[31].

Table 5: ^1H NMR data (δ , ppm) of NAT ligand.

Compound	1H,NH	Naphthalene	3H,CH ₃
NAT	8.81	7.70 – 7.32	1.72

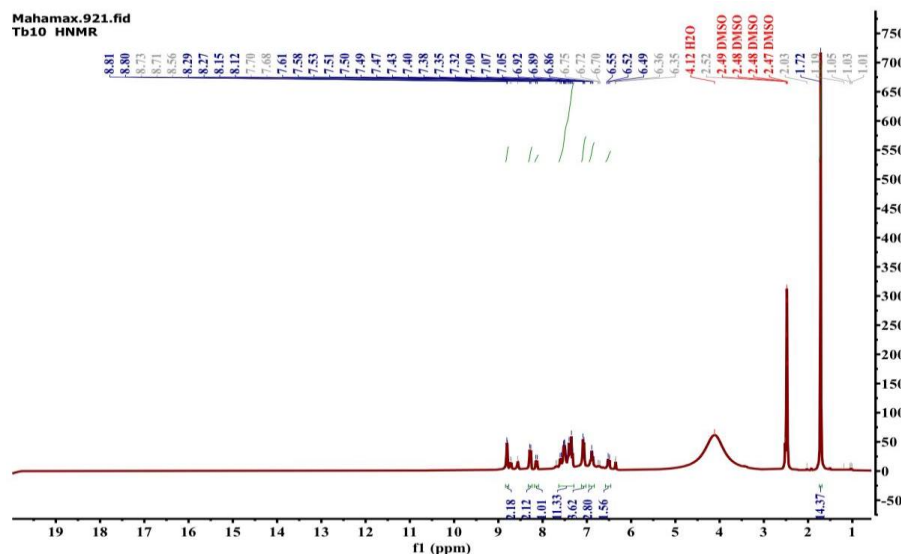


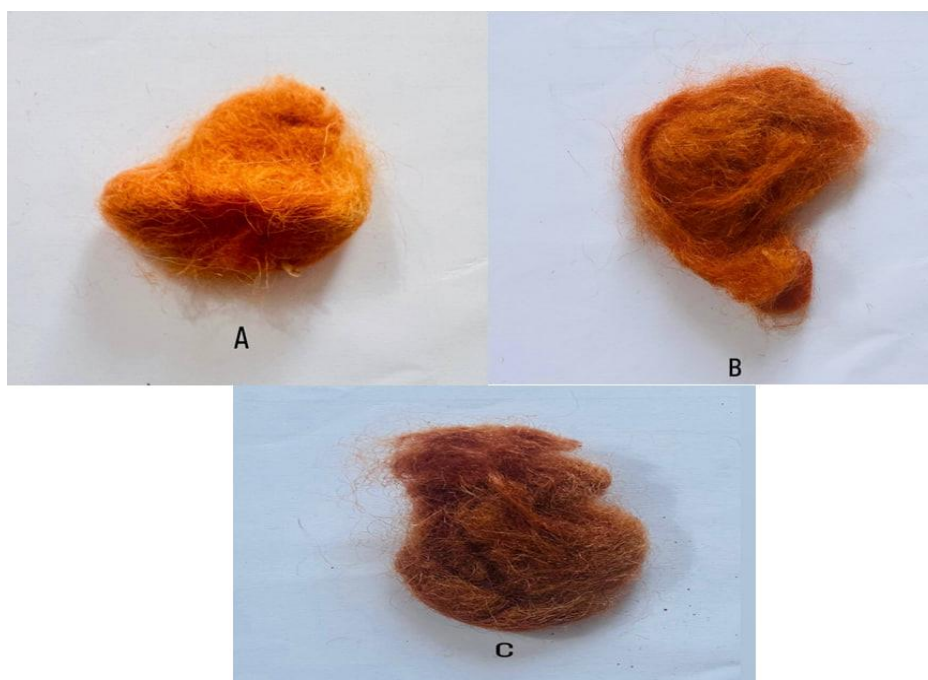
Figure 5: ^1H NMR for the ligand NAT

3.6 Dying Performance

Azo dyes are mostly wide synthetic dyes used to dye fabrics and textiles today. Compounds can be yellow, red, orange blue, or green based on their structure and o-delocalization. As a result, the intensity of the colors and the interaction of the dyes with fibres are determined by the structure and chemical formula of both the dye compound and the textile. Azo-dyes, the structural formula that confers color is the azo ($-\text{N}=\text{N}-$) group' and dye attachment to the fiber is caused by salt production between the dye's and fiber's ionic groups [32]. The absorption rate and depth of a material are influenced by factors such as the metal type, its oxidation state, the concentration in a solution, pH, time, temperature, and other factors. Notably, under alkaline pH conditions, coordination linkages can be formed by the nitrogen atoms of amide and amino groups [33]. The outcomes for the chosen complexes were also compared on a grayscale, where 4-5 are regarded as good, 3 are average, and 1-2 are not good. Iraqi specification No.175 for woollen textile at (260°C) for 30 minutes, a fixative was used to dye the models [Figure 6]. The textiles' ability to maintain their color after being washed with soap powder at a 5% concentration was examined. The material's superior resistance to both wet and dry abrasion and superior light resistance to staining and color change. The result listed in Table 6 shows that both ligand (NAT) and its complexes are considered good dyes, characterized by their color stability to washing, friction, and heat.

Table 6: Results of coloring and varied fastness features of some synthesized azo compounds on wool textile

Compound	Color	Colorfastness of fabrics According Gray scale	The result according to the measurement of the quality control device and according to Standard No. (175)
NAT	TRAFIC ORANGE	3	average and acceptable
Ag-NAT	CLAY BROWN	4	good and acceptable
Cu-NAT	TRAFIC ORANGE	3	average and acceptable

**Figure 6:** The dyes of the ligand (NAT) and other complexes (A) NAT (B) $[\text{Ag}(\text{NAT}) (\text{H}_2\text{O})_2]\text{NO}_3 \cdot 10\text{H}_2\text{O}$ (c) $[\text{Cu}(\text{NAT}) (\text{H}_2\text{O})_2] \text{Cl}_2 \cdot 10\text{H}_2\text{O}$

3.7 The acid-base indicators of the ligand (NAT)

Azo dyes that display different colors in solutions at various pH levels are referred to as acid-base indicators. These indicators are commonly utilized in acid-base titrations to determine the equivalence point. They undergo a noticeable color change when the pH shifts. Out of all the options, azo dyes are the most commonly used chemical compounds for acid-base indicators because they can change color when the pH level changes [34, 35]. Table 7 presents data related to acid-base titrations for evaluating the indicator properties of the ligand (NAT), while [Figure 7] illustrates the azo dye solutions in acidic or basic conditions.

Table 7: All data for acid-base indicator for the ligand (NAT).

No	Volume of acid	Volume of NaOH	Volume of NaHCO ₃	Color in acid	Color in base
1	(HCl) 2 ml	5 ml	-----	Yellow	Redish pink
2	(CH ₃ COOH)1ml	6 ml	-----	Brown	Red
3	(HCl) 5.5ml	-----	5.5 ml	Yellow	Red
4	(CH ₃ COOH)5.8ml	-----	6.2 ml	Brown	Red



Figure 7: variation in color for the azo ligand (A) HCl with NaOH (B) HCl with NaHCO_3 (C) CH_3COOH with NaHCO_3 (D) CH_3COOH with NaOH

Conclusion

This study involved the synthesis and analysis of the thymine-based azo ligand 5-methyl-6-((4-nitronaphthalene-1-yl) diazenyl) pyrimidine-2,4(1H,3H)-dione (NAT) and its complexes with Ag(I) and Cu(II). It was confirmed that the molecular formulas of the resulting complexes are $[\text{Ag}(\text{NAT})(\text{H}_2\text{O})_2]\text{NO}_3 \cdot 10\text{H}_2\text{O}$ and $[\text{Cu}(\text{NAT})(\text{H}_2\text{O})_2]\text{Cl}_2 \cdot 10\text{H}_2\text{O}$ through various spectroscopic and analytical techniques, and we proposed that these complexes exhibit tetrahedral geometries. The chelation occurred via the nitrogen atoms found in the azo and pyrimidine groups. Molar conductivity studies indicated that both complexes function as electrolytes. Additionally, we evaluated the dyeing properties of NAT and its metal complexes on wool fabric, which yielded impressive results, showcasing strong resistance to wear, heat, and washing, along with vibrant and glossy colors. Further studies were conducted to evaluate the NAT compound and its complexes for possible indicator applications. These findings highlight the versatile applications of NAT and its complexes in both dyeing and analytical contexts, underscoring their stability and effectiveness.

References

- [1] S. Benkhaya, S. M'rabet, and A. El Harfi, "Classifications, properties, recent synthesis and applications of azo dyes," *Heliyon*, vol. 6, no. 1, 2020.
- [2] L. D. Ardila-Leal, R. A. Poutou-Piñales, A. M. Pedroza-Rodríguez, and B. E. Quevedo-Hidalgo, "A brief history of colour, the environmental impact of synthetic dyes and removal by using laccases," *Molecules*, vol. 26, no. 13, p. 3813, 2021.
- [3] N. S. Al-Obaidi, O. D. A. Sattar, F. F. Hadi, A. S. Ali, and B. T. Zaki, "Synthesis and characterization of some azo dyes derived from 4-aminoacetophenone, 1, 4 phenylene diamine and studying its dyeing performance and antibacterial activity," *Journal of Biochemical Technology*, vol. 9, no. 4–2018, pp. 33–42, 2018.
- [4] D. R. C. Matazo, R. A. Ando, A. C. Borin, and P. S. Santos, "Azo–Hydrazone Tautomerism in Protonated Aminoazobenzenes: Resonance Raman Spectroscopy and Quantum-Chemical Calculations," *Journal of Physical Chemistry A*, vol. 112, no. 19, pp. 4437–4443, 2008.
- [5] F. Bureš, "Fundamental aspects of property tuning in push–pull molecules," *The Royal Society of Chemistry*, vol. 4, no. 102, pp. 58826–58851, 2014.
- [6] J. Del Nero, R. E. De Araujo, A. S. L. Gomes, and C. P. De Melo, "Theoretical and experimental investigation of the second hyperpolarizabilities of methyl orange," *The Journal of Chemical Physics*, vol. 122, no. 10, 2005.

- [7] R. Belcher, A. M. G. Macdonald, and E. Parry, "On mohr's method for the determination of chlorides," *Analytica Chimica Acta*, Volume 16, 1957, Pages 5, vol. 16, pp. 524–529, 1957.
- [8] L. H. Abdel-Rahman, A. M. Abu-Dief, R. M. El-Khatib, and S. M. Abdel-Fatah, "Some new nano-sized Fe (II), Cd (II) and Zn (II) Schiff base complexes as precursor for metal oxides: Sonochemical synthesis, characterization, DNA interaction, in vitro antimicrobial and anticancer activities," *Bioorganic Chemistry*, vol. 69, pp. 140–152, 2016.
- [9] H. M. Salh and T. H. Al-Noor, "Preparation, Structural Characterization and Biological Activities of Curcumin-Metal (II)-L-3, 4-dihydroxyphenylalanin (L-dopa) complexes," *Ibn Al-Haitham Journal for Pure and Applied Sciences*, vol. 36, no. 1, pp. 170–185, 2023.
- [10] A. M. Al-Azzawi and E. K. Jassem, "Synthesis and characterization of several new succinimides linked to phenyl azo benzothiazole or thiazole moieties with expected biological activity," *Iraqi Journal of Science*, pp. 534–544, 2016.
- [11] A. M. N. Khaleel and M. I. Jaafar, "Synthesis and characterization of boron and 2-aminophenol Schiff base ligands with their Cu (II) and Pt (IV) complexes and evaluation as antimicrobial agents," *Oriental Journal of Chemistry*, vol. 33, no. 5, pp. 2394–2404, 2017.
- [12] R. K. H. Al-Daffay and A. A. S. Al-Hamdani, "Synthesis, Characterization, and Thermal Analysis of a New Acidicazo Ligand's Metal Complexes," *Baghdad Science Journal*, vol. 20, no. 1, p. 121, 2023.
- [13] P. Noriega, G. Gortaire, and E. Osorio, "Mass Spectrometry and Its Importance for the Analysis and," *Natural Drugs from Plants*, p. 33, 2022.
- [14] W. A. Mahmoud, A. A. M. Ali, and T. A. Kareem, "Preparation and spectral characterization of new azo imidazole ligand 2-[(2-cyano phenyl) Azo]-4, 5-Diphenyl imidazole and its complexes with Co (II), Ni (II), Cu (II), Zn (II), Cd (II) and Hg (II) ions," *Baghdad Science Journal*, vol. 12, no. 1, pp. 96–109, 2015.
- [15] F. Karçı, A. Demirçalı, İ. Şener, and T. Tilki, "Synthesis of 4-amino-1H-benzo [4, 5] imidazo [1, 2-a] pyrimidin-2-one and its disperse azo dyes. Part 1: Phenylazo derivatives," *Dyes and Pigments*, vol. 71, no. 2, pp. 90–96, 2006.
- [16] M. A. Hissam, Z. Ngaini, N. H. Zamakshshari, F. N. A. M. Hejemi, F. S. Arni, and A. N. A. Halim, "Synthesis and molecular docking simulation on the antimicrobial effects of halogenated vanillin-azo dyes and schiff base derivatives," *Discover Applied Sciences*, vol. 6, no. 6, p. 325, 2024.
- [17] A. E. Fadhil and A. K. Abbas, "Antioxidant, Antimicrobial and Spectroscopic Discussion of Guanine Azo Ligand with Cu (II) and Ag (I) Complexes," *Ibn Al-Haitham Journal for Pure and Applied Sciences*, vol. 36, no. 4, pp. 207–220, 2023.
- [18] A. A. Ali, R. M. Al-Hassani, D. H. Hussain, A. M. Rheima, and H. S. Meteab, "Synthesis, spectroscopic, characterization, pharmacological evaluation, and cytotoxicity assays of novel nano and micro scale of copper (II) complexes against human breast cancer cells.," *Drug Invention Today*, vol. 14, no. 1, 2020.
- [19] S. S. Mahmoud and A. M. N. Khaleel, "Synthesis, Identification and Biological Study of New Pharmaceutical Model Based on Amino Acids with Some of Its Complexes," *Iraqi Journal of Science*, pp. 5501–5516, 2023.
- [20] A. Rehab Abd Al-husseinDabish, "Synthesis and Spectral Studies of Some New Complexes Containing Azo Ligand with Anticancer, Antibacterial and Dyeing Performance.," *Annals of the Romanian Society for Cell Biology*, pp. 7968–8006, 2021.
- [21] K. J. Al-Adilee and H. Hesson, "Synthesis, identification, structural, studies and biological activity of some transition metal complexes with novel heterocyclic azo-Schiff base ligand derived from benzimidazole," *Journal of Chemical and Pharmaceutical Research*, vol. 7, no. 8, pp. 89–103, 2015.
- [22] N. M. Mallikarjuna, J. Keshavayya, M. R. Maliyappa, R. A. S. Ali, and T. Venkatesh, "Synthesis, characterization, thermal and biological evaluation of Cu (II), Co (II) and Ni (II) complexes of azo dye ligand containing sulfamethaxazole moiety," *Journal of Molecular Structure*, vol. 1165, pp. 28–36, 2018.
- [23] E. Merino, "Synthesis of azobenzenes: the coloured pieces of molecular materials," *Chemical Society Reviews*, vol. 40, no. 7, pp. 3835–3853, 2011.

- [24] M. Gaber, N. El-Wakiel, and O. M. Hemed, "Cr (III), Mn (II), Co (II), Ni (II) and Cu (II) complexes of 7-((1H-benzo [d] imidazol-2-yl) diazenyl)-5-nitroquinolin-8-ol. synthesis, thermal, spectral, electrical measurements, molecular modeling and biological activity," *Journal of Molecular Structure*, vol. 1180, pp. 318–329, 2019.
- [25] A. K. Abbas and A. E. Fadhil, "Preparation, Structural Identification, and Biomedical Evaluation of Some New Complexes," *Indonesian Journal of Chemistry*.
- [26] M. Bouhdada and M. E. L. Amame, "Synthesis, characterization and spectroscopic properties of the hydrazodye and new hydrazodye-metal complexes," *Journal of Molecular Structure*, vol. 1150, pp. 419–426, 2017.
- [27] K. D. Patel and H. S. Patel, "Synthesis, spectroscopic characterization and thermal studies of some divalent transition metal complexes of 8-hydroxyquinoline," *Arabian Journal of Chemistry*, vol. 10, pp. S1328–S1335, 2017.
- [28] J. R. Štoček and M. Dračinský, "Tautomerism of guanine analogues," *Biomolecules*, vol. 10, no. 2, p. 170, 2020.
- [29] H. A. Bayoumi, A.-N. M. A. Alaghaz, and M. S. Aljahdali, "Cu (II), Ni (II), Co (II) and Cr (III) complexes with N2O2-chelating schiff's base ligand incorporating azo and sulfonamide moieties: spectroscopic, electrochemical behavior and thermal decomposition studies," *International Journal of Electrochemical Science*, vol. 8, no. 7, pp. 9399–9413, 2013.
- [30] P. Singh, A. Kumar, S. Kaur, and A. Singh, "Thymidylate synthase inspired biomodel reagent for the conversion of uracil to thymine," *Chemical Communications*, vol. 51, no. 49, pp. 9961–9964, 2015.
- [31] R. Patil, M. Jadhav, S. Salunke-Gawali, D. N. Lande, S. P. Gejji, and D. Chakravarty, "1H and 13C NMR chemical shifts of 2-n-alkylamino-naphthalene-1, 4-diones," *Heliyon*, vol. 7, no. 1, 2021.
- [32] M. Kareem Samad, "Synthesis, Characterization and dyeing performance studies of some azo dyes derived from m-phenylenediamine," *Zanco Journal of Pure and Applied Sciences*, vol. 28, no. 6, pp. 148–157, 2017.
- [33] D. J. Jasim and A. K. Abbas, "Synthesis, identification, antibacterial, medical and dyeing performance studies for azo-sulfamethoxazole metal complexes," *Eurasian Chemical Communications*, vol. 4, no. 1, pp. 16–40, 2022.
- [34] J. Naime, M. S. Al Mamun, M. A. S. Aly, M. Maniruzzaman, M. M. R. Badal, and K. M. R. Karim, "Synthesis, characterization and application of a novel polyazo dye as a universal acid–base indicator," *The Royal Society of Chemistry*, vol. 12, no. 43, pp. 28034–28042, 2022.
- [35] S. M. H. Al-Majidi and M. G. A. Al-Khuzai, "Synthesis and characterization of new azo compounds linked to 1, 8-naphthalimide and studying their ability as acid-base indicators," *Iraqi Journal of science*, pp. 2341–2352, 2019.